# **PCCP**



PAPER View Article Online
View Journal | View Issue



Cite this: *Phys. Chem. Chem. Phys.*, 2016, **18**, 6077

Received 27th November 2015, Accepted 26th January 2016

DOI: 10.1039/c5cp07313h

www.rsc.org/pccp

# Active performance of tetrahedral groups to SHG response: theoretical interpretations of Ge/Si-containing borate crystals†

Linping Li,<sup>ab</sup> Zhihua Yang,<sup>b</sup> Bing-Hua Lei,<sup>b</sup> Qingrong Kong,<sup>b</sup> Ming-Hsein Lee,<sup>c</sup> Bingbing Zhang,<sup>b</sup> Shilie Pan<sup>b</sup> and Jun Zhang\*<sup>a</sup>

As potential candidates for deep-UV nonlinear optical (NLO) crystals, borosilicates and borogermanates, which contain NLO-active groups such as B-O, Si-O and Ge-O, have fascinated many scientists. The crystal structures, electronic structures and optical properties of seven borates in different B/R (R = Si, Ge) ratios have been studied using DFT methods. Through the SHG-density, we find that besides the recognized contribution of the  $\pi$ -conjugation configuration of BO<sub>3</sub> to second harmonic generation (SHG), the tetrahedra have a non-negligible influence. This is because the non-bonding p orbitals of the bridging oxygen in the tetrahedra are observably closer to the Fermi level than those in BO<sub>3</sub>, which is observed in the PDOS of Rb<sub>4</sub>Ge<sub>3</sub>B<sub>6</sub>O<sub>17</sub> and RbGeB<sub>3</sub>O<sub>7</sub>. This conclusion would be very meaningful in the understanding of the relationship between the crystal structure and nonlinear optical properties.

#### 1. Introduction

With the development of laser micromachining, laser communication, and modern scientific instruments, the requirement for NLO crystals is growing rapidly. 1-3 So far, commercialized optical crystals such as β-BaB<sub>2</sub>O<sub>4</sub> (BBO), LiB<sub>3</sub>O<sub>5</sub> (LBO)<sup>5</sup> and CsLiB<sub>6</sub>O<sub>10</sub> (CLBO)<sup>6</sup> have been used for these applications, and potential candidates such as Pb<sub>17</sub>O<sub>8</sub>Cl<sub>18</sub> (POC), Ba<sub>23</sub>Ga<sub>8</sub>Sb<sub>2</sub>S<sub>38</sub>, Ba<sub>4</sub>B<sub>11</sub>O<sub>20</sub>F (BBOF),2 and K3B6O10Cl (KBOC)9 are emerging, but it is still challenging to get "wanted" NLO materials with conditions satisfying a "large SHG response", "laser damage threshold", and "short UV cut-off". According to anionic group theory, 10 the main non-linearity of a crystal is the geometrical superposition of the microscopic second-order susceptibility of the constituent NLO-active anionic groups. Some well-known NLO-active anion groups, such as BO<sub>3</sub>, CO<sub>3</sub>, and NO<sub>3</sub> triangles with  $\pi$ -conjugation configurations, <sup>11</sup> MO<sub>6</sub> octahedra (M = Mo<sup>6+</sup>, W<sup>6+</sup>, Nb<sup>5+</sup>, and V<sup>5+</sup>) with  $d^0$  transition metal ions,  $d^{12-14}$  and  $d^{12}$  and  $d^{12}$  and  $d^{12}$  $(T = Pb^{2+}, Bi^{3+})$  with active lone pairs, <sup>15,16</sup> have been explored as

Ge/Si-containing alkaline, alkaline earth and rare earth metal borates are representative because of the rich structures involved in combining groups of Ge/Si-O tetrahedra and B-O groups, and such borates have fascinated many material scientists to study their optical properties due to their promising uses in optical equipment. 20-24 Studies show that Ge/Si-containing borate crystals have the properties of deep-UV cut-off edges.<sup>25</sup> Up to now, a series of Ge/Si-containing borates have been synthesized, such as  $Cs_2GeB_4O_9$ , <sup>26</sup>  $Cs_2B_4SiO_9$  <sup>27</sup> and  $LaBGeO_5$ , <sup>28</sup> which all have potential for application in deep-UV second-order nonlinearoptical crystalline materials based on their moderate SHG responses and short cut-off edges under 200 nm.26,28-30 In addition to this, various frameworks built of B-O and R-O (R = Si, Ge) are potent factors to obtain excellent materials. Some investigators reported that the molar ratio of B/R can affect the structural type of such composite borates. 31 In B-rich R-containing borates where B/R > 1, the basic B-O units tend to condense into rings and then connect with RO4, such as in RbGeB<sub>3</sub>O<sub>7</sub><sup>20</sup> with a B/Ge ratio of 3/1 and Rb<sub>2</sub>GeB<sub>4</sub>O<sub>9</sub><sup>20</sup> with a B/Ge ratio of 4/1, in which the  $B_3O_7$  or  $B_4O_9$  BBUs combined with GeO4 by sharing the vertices of oxygen atoms to form a B-Ge-O connection mode. BO4 and RO4 structural motifs are found in low polymer borosilicate LaBRO<sub>5</sub><sup>32,33</sup> with a B/Si ratio

feasible NLO candidates. A crystal containing one or more NLO active groups may possess a stronger NLO effect, typical examples are  $Pb_2B_5O_9I$  with  $13.5 \times KDP^{16}$  and  $Pb_2(BO_3)(NO_3)$  with  $9 \times KDP$ . However, the  $BO_3$  group, possessing both wide transparency and large SHG effects, is still one of the best structural units for deep-UV NLO materials. The structural structural units for deep-UV NLO materials.

<sup>&</sup>lt;sup>a</sup> School of Physics Science and Technology, Xinjiang University, Urumqi 830046, China. E-mail: zhj@xju.edu.cn

 <sup>&</sup>lt;sup>b</sup> Xinjiang Technical Institute of Physics & Chemistry, Chinese Academy of Sciences,
 40-1 South Beijing Road, Urumqi 830011, China. E-mail: zhyang@ms.xjb.ac.cn
 <sup>c</sup> Department of Physics, Tamkang University, Taipei 25137, Taiwan

 $<sup>\</sup>dagger$  Electronic supplementary information (ESI) available: Different R–O patterns of KBGeO $_6$  and Li $_4$ BaySi $_8$ O $_2$ a; band structures of KBGe $_2$ O $_6$ , Li $_4$ BaySi $_8$ O $_2$ a, LaBSiO $_5$ , LaBGeO $_5$ , Rb $_4$ Ge $_3$ BayGo $_7$ , RbGeBayO $_7$  and Rb $_2$ GeBayO $_9$ ; density of state (DOS) of KBGe $_2$ Oa, Li $_4$ BaySiayO $_4$ , LaBSiO $_5$ , LaBGeO $_5$ , Rb $_4$ Ge $_3$ BayGo $_7$ , RbGeBayO $_7$  and Rb $_2$ GeBayO $_7$ , RbGeBayO $_7$  and Rb $_2$ GeBayO $_7$ , RbGeBayO $_7$  and Rb $_2$ GeBayO $_7$ . See DOI: 10.1039/c5cp07313h

of 1, and they form B–O–R six-membered rings which are formed by sharing the vertices of oxygen atoms. Meanwhile, in the R-rich case, the basic R–O units are in a chain or a cluster instead of a ring, and the neighbouring R–O chains or clusters share terminal O atoms with BO $_4$  groups and cations to form the 3D framework, typical examples of this are  $\text{Li}_4\text{B}_4\text{Si}_8\text{O}_{24}^{\phantom{24}34}$  and  $\text{KBGe}_2\text{O}_6.^{22}$ 

Recently, only tetrahedral basic building unit (BBU) containing materials, such as  $BPO_4$ ,  $LiBGeO_4$  and  $Ba_3P_3O_{10}X$  (X = Cl, Br), have been reported to have considerable SHG, 1,29,35 implying that tetrahedral materials could also have a SHG response comparable with that of compounds that contain BO3 groups. It is well known that tetrahedral structures possess shorter UV cut-off edges than BO<sub>3</sub>, such as the cut-off edges of BPO<sub>4</sub><sup>35</sup> and LaBGeO<sub>5</sub>, 30 which are below 134 nm and 193 nm, respectively. These characteristics make this kind of material a potential NLO material for deep-UV if the SHG response is considerable. In fact, some tetrahedra such as  $(AO_4)^{3-}$  (A = P, Si, Ge and V) have been proven to have non-negligible contributions to the SHG response in the borate structures MBPO<sub>5</sub> (M = Sr, Ba), LaBRO<sub>5</sub> (R = Si, Ge) and Na<sub>3</sub>VO<sub>2</sub>B<sub>6</sub>O<sub>11</sub>. <sup>12,36,37</sup> However, when and why such tetrahedra play an important role remains unclear. To address this question, it is necessary to investigate the relationship between the electronic properties of the anionic groups (including tetrahedra and triangles) and the optical properties, which is meaningful and vital for exploring and synthesizing various new composite NLO materials used for UV/deep-UV wavelengths.

In this work, seven Ge/Si-containing alkaline, alkaline earth and rare earth metal borates with different B–R ratios, ranging from B-rich to R-rich (Rb<sub>2</sub>GeB<sub>4</sub>O<sub>9</sub>,<sup>20</sup> RbGeB<sub>3</sub>O<sub>7</sub>,<sup>20</sup> Rb<sub>4</sub>Ge<sub>3</sub>B<sub>6</sub>O<sub>17</sub>,<sup>20</sup> LaBSiO<sub>5</sub>,<sup>33</sup> LaBGeO<sub>5</sub>,<sup>32</sup> Li<sub>4</sub>B<sub>4</sub>Si<sub>8</sub>O<sub>24</sub>,<sup>34</sup> KBGe<sub>2</sub>O<sub>6</sub>,<sup>22</sup>), are studied. The relationship between the B–R ratio and the crystal structures, electronic properties, energy bands, and especially the optical properties are studied systematically. The SHG-density method is used to characterise the SHG response of the electrons in groups and atoms. The results show that RO<sub>4</sub> and BO<sub>4</sub> also take important roles in the SHG effect in compounds containing BO<sub>3</sub>, particularly the oxygen between tetrahedra. This is because the non-bonding p orbitals of the bridging oxygens in the tetrahedra are closer to the Fermi level than the conjugated  $\pi$  orbital in BO<sub>3</sub>, which was observed from analyzing the PDOS.

# 2. Computational conditions and theories

#### 2.1. Electronic structures and linear optical properties

The electronic and band structures of  $Rb_2GeB_4O_9$ ,  $RbGeB_3O_7$ ,  $Rb_4Ge_3B_6O_{17}$ ,  $LaBSiO_5$ ,  $LaBGeO_5$ ,  $Li_4B_4Si_8O_{24}$ , and  $KBGe_2O_6$  are calculated using plane-wave pseudopotential density functional theory (DFT) implemented in a CASTEP module. <sup>38,39</sup> For LaBSiO<sub>5</sub>,  $LaBGeO_5$  and  $Rb_2GeB_4O_9$ , the generalized gradient approximation (GGA) with the Perdew–Burke–Ernzerhof (PBE)<sup>40</sup> functional is selected as the exchange–correlation potential and ultrasoft pseudopotentials (USPs)<sup>41</sup> are used for all chemical elements. The local-density approximation (LDA) for

the exchange–correlation potential energy and norm-conserving pseudopotential (NCP) $^{40,41}$  are used for KBGe<sub>2</sub>O<sub>6</sub>, Li<sub>4</sub>B<sub>4</sub>Si<sub>8</sub>O<sub>24</sub>, Rb<sub>4</sub>Ge<sub>3</sub>B<sub>6</sub>O<sub>17</sub> and RbGeB<sub>3</sub>O<sub>7</sub>. The valence electron configurations for the diverse electron orbital pseudopotentials are chosen as Li 2s<sup>1</sup>, K 3s<sup>2</sup> 3p<sup>6</sup> 4s<sup>1</sup>, La 5d<sup>1</sup> 6s<sup>2</sup>, Rb 4s<sup>2</sup> 4p<sup>6</sup> 5s<sup>1</sup>, B 2s<sup>2</sup> 2p<sup>1</sup>, Si 3s<sup>2</sup> 3p<sup>2</sup>, Ge 4s<sup>2</sup> 4p<sup>2</sup>, and O 2s<sup>2</sup> 2p<sup>4</sup>. The plane-wave energy cutoff is set at 830 eV for KBGe<sub>2</sub>O<sub>6</sub>, Li<sub>4</sub>B<sub>4</sub>Si<sub>8</sub>O<sub>24</sub>, Rb<sub>4</sub>Ge<sub>3</sub>B<sub>6</sub>O<sub>17</sub> and RbGeB<sub>3</sub>O<sub>7</sub>; 390 eV for LaBSiO<sub>5</sub> and LaBGeO<sub>5</sub>; and 380 eV for Rb<sub>2</sub>GeB<sub>4</sub>O<sub>9</sub>. The Monkhorst–Pack *k*-point is sampled with a separation of less than 0.04 Å<sup>-1</sup> and the other parameters and convergent criteria are set to the default values of the CASTEP code.

A so-called scissors operation  $^{42,43}$  is used in the evaluation of optical properties. The gap correction  $\varDelta$  is the difference between the calculated band gap and the experimental one. To determine the refractive index along the principal axes of the seven compounds, the optical permittivity tensor elements are gathered and the diagonalization transformation is performed. After rotation operation, the linear optical properties of the seven compounds are calculated using the principal dielectric axis coordinate system.

#### 2.2. Methods for calculating non-linear optical properties

At a zero frequency limit, the SHG coefficients are calculated using the so-called length-gauge formalism derived by Aversa and Sipe.  $^{45}$  The static second order susceptibilities  $\chi^{(2)}_{\alpha\beta\gamma}$  can be written as,  $^4$ 

$$\chi_{\alpha\beta\gamma}^{(2)} = \chi_{\alpha\beta\gamma}^{(2)}(VE) + \chi_{\alpha\beta\gamma}^{(2)}(VH),$$
(1)

Virtual-electrons (VEs) can be ascribed as,

$$\chi_{\alpha\beta\gamma}^{(2)}(\text{VE}) = \frac{e^3}{2\hbar m^3} \sum_{\text{vcc'}} \int \frac{d^3k}{4\pi^3} P(\alpha\beta\gamma) \text{Im} \left[ P_{\text{cv}}^{\alpha} P_{\text{cc'}}^{\beta} P_{\text{c'v}}^{\gamma} \right] \times \left( \frac{1}{\omega_{\text{cv}}^3 \omega_{\text{vc'}}^2} + \frac{2}{\omega_{\text{vc}}^4 \omega_{\text{c'v}}} \right), \tag{2}$$

Virtual-holes (VHs) can be ascribed as,

$$\chi_{\alpha\beta\gamma}^{(2)}(VH) = \frac{e^3}{2\hbar m^3} \sum_{vv'c} \int \frac{d^3k}{4\pi^3} P(\alpha\beta\gamma) Im \left[ P_{vv'}^{\alpha} P_{cv'}^{\beta} P_{cv}^{\gamma} \right] \times \left( \frac{1}{\omega_{cv}^3 \omega_{v'c}^2} + \frac{2}{\omega_{vc}^4 \omega_{cv'}} \right).$$
(3)

where  $\alpha$ ,  $\beta$ , and  $\gamma$  are Cartesian components, v and v' denote valence bands, c and c' refer to conduction bands, and  $P(\alpha\beta\gamma)$  denotes full permutation. The band energy difference and momentum matrix elements are denoted as  $\hbar\omega_{ij}$  and  $P^{\alpha}_{ij}$ , respectively. The two-band process was proved to be exactly zero which can be neglected in earlier work.

The band-resolved method  $^{47,48}$  is used. By using this method, the effective values of individual electronic states in the SHG coefficients can be divided into occupied and unoccupied bands, and the orbital contributions of total  $\chi^{(2)}$  can be calculated. Furthermore, the integral SHG contribution of the corresponding energy region and the contribution of the valence bands and conduction bands can be obtained. The SHG-density method  $^{49}$  is

**PCCP** Paper

performed using the effective SHG of each band (occupied and unoccupied) as the weighting coefficient (after being normalized with the total VE or VH  $\chi^{(2)}$  value) by summing together all of the probability densities of the occupied or unoccupied states. The SHG density can hence ensure that the quantum states irrelevant to SHG will not be shown in the occupied or unoccupied SHGdensity, and the resulting distribution of such density highlights the origin of SHG.

# 3. Anionic group frameworks with different B/R ratios

The B-R connection patterns of KBGe<sub>2</sub>O<sub>6</sub> (ICSD281258), Li<sub>4</sub>B<sub>4</sub>Si<sub>8</sub>O<sub>24</sub> (ICSD90849), LaBRO<sub>5</sub> (ICSD83397, ICSD39262), Rb<sub>4</sub>Ge<sub>3</sub>B<sub>6</sub>O<sub>17</sub> (ICSD261334), RbGeB<sub>3</sub>O<sub>7</sub> (ICSD261332), and Rb<sub>2</sub>GeB<sub>4</sub>O<sub>9</sub> (ICSD261333) are shown in Fig. 1. It is obvious that the BBUs of the B-rich structures Rb<sub>4</sub>Ge<sub>3</sub>B<sub>6</sub>O<sub>17</sub>, RbGeB<sub>3</sub>O<sub>7</sub> and Rb<sub>2</sub>GeB<sub>4</sub>O<sub>9</sub> are BO<sub>3</sub>, BO<sub>4</sub> and RO<sub>4</sub>, and B-O forms B<sub>3</sub>O<sub>8</sub>, B<sub>3</sub>O<sub>7</sub> and B<sub>4</sub>O<sub>9</sub> rings, respectively. The B-O rings and RO<sub>4</sub> are interlinked through sharing the vertices of oxygen atoms to form the B-O-R frameworks. In the R-rich case with a B/R ratio of 1/2, the BBUs of KBGe<sub>2</sub>O<sub>6</sub> and Li<sub>4</sub>B<sub>4</sub>Si<sub>8</sub>O<sub>24</sub> are BO<sub>4</sub> and RO<sub>4</sub>, no BO<sub>3</sub> exists. Although the two compounds have the same B/R ratio, their R-O patterns are different. For KBGe<sub>2</sub>O<sub>6</sub>, the  $[Ge_2O_7]^{4-}$ dimers formed by the condensation of [GeO<sub>4</sub>]<sup>3-</sup> units are linked by the topmost O atoms to form a chain along the a axis. While there

are eight different possible coordination surroundings, the Si-O groups form four diverse  $[SiO_3]_{\infty}$  chains along the a axis in Li<sub>4</sub>B<sub>4</sub>Si<sub>8</sub>O<sub>24</sub>, as described in Fig. S1 (ESI†). The neighbouring chains in the R-rich KBGe<sub>2</sub>O<sub>6</sub> and Li<sub>4</sub>B<sub>4</sub>Si<sub>8</sub>O<sub>24</sub> compounds are all connected by BO4 groups through sharing vertical oxygens to form frameworks of anionic groups. The difference in BBUs results in diverse symmetries of these two compounds, these are orthorhombic P2<sub>1</sub>2<sub>1</sub>2<sub>1</sub> for KBGe<sub>2</sub>O<sub>6</sub> and monoclinic P2<sub>1</sub> for Li<sub>4</sub>B<sub>4</sub>Si<sub>8</sub>O<sub>24</sub>. This may be due to the larger radius of K<sup>+</sup> and Ge<sup>4+</sup> cations, and the different coordination environments of K<sup>+</sup> and Li<sup>+</sup>. For the case of a B/R ratio of 1, the compound LaBRO<sub>5</sub> shows a [BO<sub>3</sub>]<sub>∞</sub> spiral chain type formed by BO<sub>4</sub> groups, in which the R atoms are connected with two neighbouring BO<sub>4</sub> groups, and the neighbouring chains are linked by La<sup>3+</sup> along the z axis to form 3D frameworks. From this we see that there is a close relationship between the B-R ratio and the BBUs, the B-O groups change from a three-coordination to four-coordination along with a change from B-rich to R-rich.

## 4. Results and discussion

#### 4.1. Electronic structures

The calculated band gaps are shown in Fig. S2 (ESI†), KBGe<sub>2</sub>O<sub>6</sub>, LaBGeO<sub>5</sub>, Rb<sub>4</sub>Ge<sub>3</sub>B<sub>6</sub>O<sub>17</sub> and Rb<sub>2</sub>GeB<sub>4</sub>O<sub>9</sub> are indirect band gap crystals with band gaps of 3.769, 4.185, 4.330 and 4.269 eV, respectively. Li<sub>4</sub>B<sub>4</sub>Si<sub>8</sub>O<sub>24</sub>, LaBSiO<sub>5</sub> and RbGeB<sub>3</sub>O<sub>7</sub> are direct

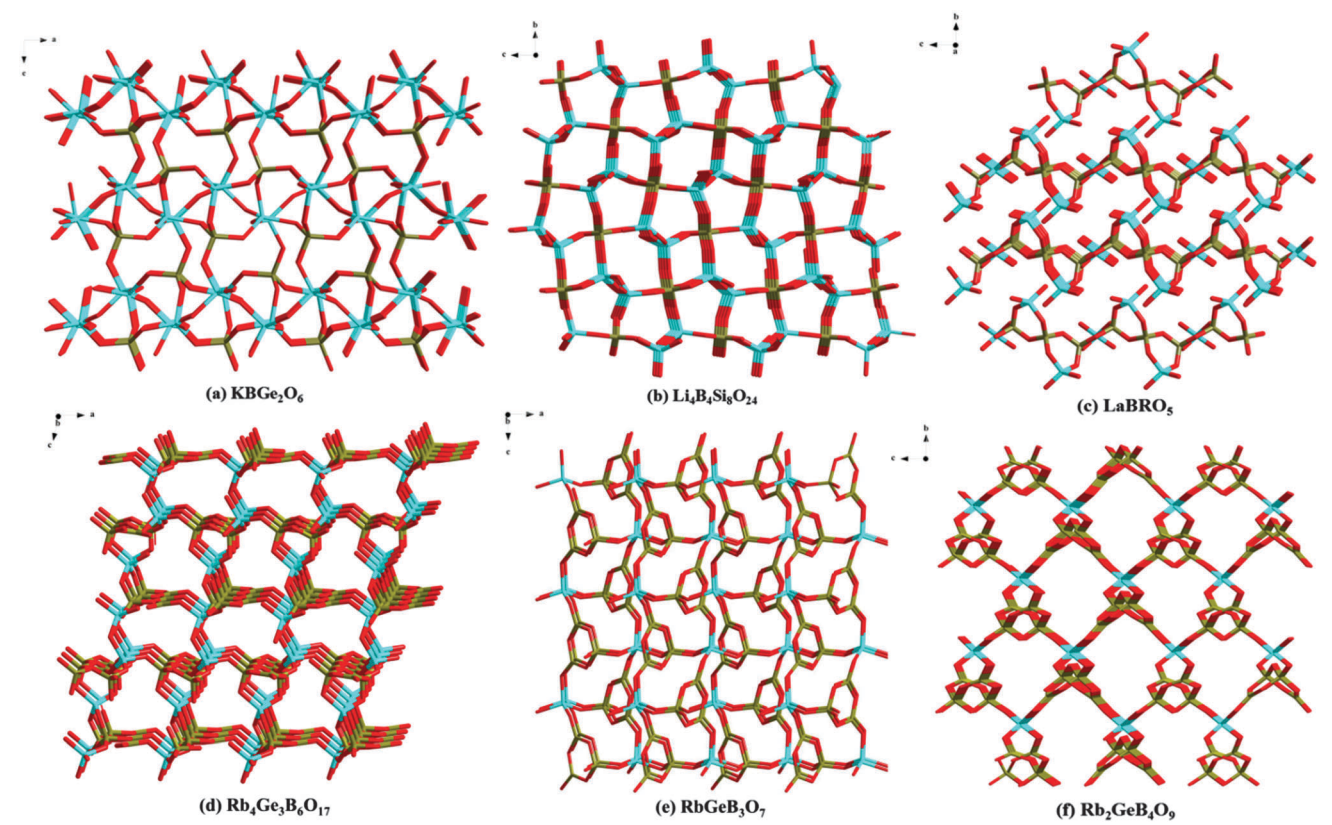


Fig. 1 Structures of anionic connection modes for the seven compounds. The "green 🔪" represents B–O groups, and the "blue 💢" represents

Paper

band gap crystals with band gaps of 5.509, 5.158 and 4.770 eV, respectively. The PDOS of KBGe<sub>2</sub>O<sub>6</sub>, Li<sub>4</sub>B<sub>4</sub>Si<sub>8</sub>O<sub>24</sub>, LaBSiO<sub>5</sub>, LaBGeO<sub>5</sub>, Rb<sub>4</sub>Ge<sub>3</sub>B<sub>6</sub>O<sub>17</sub>, RbGeB<sub>3</sub>O<sub>7</sub> and Rb<sub>2</sub>GeB<sub>4</sub>O<sub>9</sub> is demonstrated in Fig. S3 (ESI†), from which we can figure out the respective contributions of the cations and anionic groups in the near Fermi surface. In the case of the B-rich structures Rb<sub>4</sub>Ge<sub>3</sub>B<sub>6</sub>O<sub>17</sub>, RbGeB<sub>3</sub>O<sub>7</sub> and Rb<sub>2</sub>GeB<sub>4</sub>O<sub>9</sub>, the conduction bands mainly come from the 4s 4p of Ge4+, 2p of B3+, or s 4p of Rb<sup>+</sup> and 2p of O<sup>2-</sup>. For the R-rich structures KBGe<sub>2</sub>O<sub>6</sub> or Li<sub>4</sub>B<sub>4</sub>Si<sub>8</sub>O<sub>24</sub>, the p of K<sup>+</sup> or 2s of Li<sup>+</sup>, 4s 4p of Ge<sup>4+</sup> or 3s, 3p of Si<sup>4+</sup> and 2p of O<sup>2-</sup> make the main contribution to the bottom of the conduction bands. At the top of the valence bands of the seven studied compounds, the dominating positions are all occupied by the 2p orbitals of O<sup>2-</sup>. Generally speaking, for the seven compounds discussed above, the interaction of the K<sup>+</sup>, Li<sup>+</sup>, Rb<sup>+</sup> and La<sup>3+</sup> cations and the 2p orbital of O<sup>2-</sup> control the near Fermi level. Furthermore, one can see that the orbitals of B and R have changed based on different B-R ratios at the top

#### 4.2. Origin of the SHG response

of the valence band.

Both GW and hybrid functions have been adopted to study the band structures of nonlinear optic crystals, 23,24,50 but usually DFT will underestimate the band gap comparing the experimental value. The scissors operation is used to calculate the optical properties. For the seven studied compounds, the scissors operators are chosen as the difference between the calculated band gap and the experimental one or the PBE0 results, these are 2.301 eV for KBGe<sub>2</sub>O<sub>6</sub>, 2.619 eV for Li<sub>4</sub>B<sub>4</sub>Si<sub>8</sub>O<sub>24</sub>, 2.375 eV for LaBSiO<sub>5</sub>, 2.415 eV for LaBGeO<sub>5</sub>, 1.09 eV for Rb<sub>4</sub>Ge<sub>3</sub>B<sub>6</sub>O<sub>17</sub>, 2.149 eV for RbGeB<sub>3</sub>O<sub>7</sub> and 1.271 eV for Rb<sub>2</sub>GeB<sub>4</sub>O<sub>9</sub>. Taking into account the scissors operator, the calculated linear and non-linear optical properties of the seven compounds are shown in Table 1, where the calculated efficient tensors are in good agreement with the SHG response in experiments. In this table, we can see that a larger B/R ratio tends to have a stronger SHG response. According to earlier work on the origin of birefringence values<sup>51</sup> and SHG responses, 44,52 BO<sub>3</sub> may be the main source of both the large birefringence and the SHG response.

In this work, the SHG-density method is employed to analyze the electron states in three of the B-rich compounds Rb<sub>4</sub>Ge<sub>3</sub>B<sub>6</sub>O<sub>17</sub>, RbGeB<sub>3</sub>O<sub>7</sub> and Rb<sub>2</sub>GeB<sub>4</sub>O<sub>9</sub> to study the mechanism of the SHG response. The virtual-electron (VE) contributions to the total SHG coefficients are obtained using the band-resolved method, these contributions are 74.63%  $(d_{15})$ , 94.06%  $(d_{33})$  and 86.00% ( $d_{14}$ ) for Rb<sub>4</sub>Ge<sub>3</sub>B<sub>6</sub>O<sub>17</sub>, RbGeB<sub>3</sub>O<sub>7</sub> and Rb<sub>2</sub>GeB<sub>4</sub>O<sub>9</sub>, respectively. For the compound Rb<sub>4</sub>Ge<sub>3</sub>B<sub>6</sub>O<sub>17</sub>, the occupied state of VEs is occupied by bridging oxygen O9 and O10, which are the bridging oxygens of the two neighbouring BO<sub>4</sub> groups (shown in Fig. 2). The unoccupied state of VEs is taken up by the BO<sub>3</sub> groups and the bridging oxygens of GeO<sub>4</sub> and BO<sub>4</sub> (Fig. 2a). For Rb<sub>4</sub>Ge<sub>3</sub>B<sub>6</sub>O<sub>17</sub>, the non-bonding 2p orbitals of the bridging oxygens of GeO<sub>4</sub> and  $BO_4$  or  $BO_3$ , instead of those in the  $\pi$ -conjugation configuration of the BO<sub>3</sub> groups (Fig. 2b), have a considerable contribution to SHG. In the case of Rb<sub>2</sub>GeB<sub>4</sub>O<sub>9</sub>, the contributions to SHG come from BO<sub>3</sub>, BO<sub>4</sub> and GeO<sub>4</sub>, as shown in Fig. 2c. That is to say, the  $\pi$ -conjugation configuration of the BO<sub>3</sub> group is not the only contributor to the SHG response in the B-rich structures, especially in RbGeB<sub>3</sub>O<sub>7</sub>. Why do the tetrahedra such as BO<sub>4</sub>, SiO<sub>4</sub> or GeO<sub>4</sub> make a significant contribution to the SHG response? To clear up this question, we have analysed the electron states in the near Fermi surface.

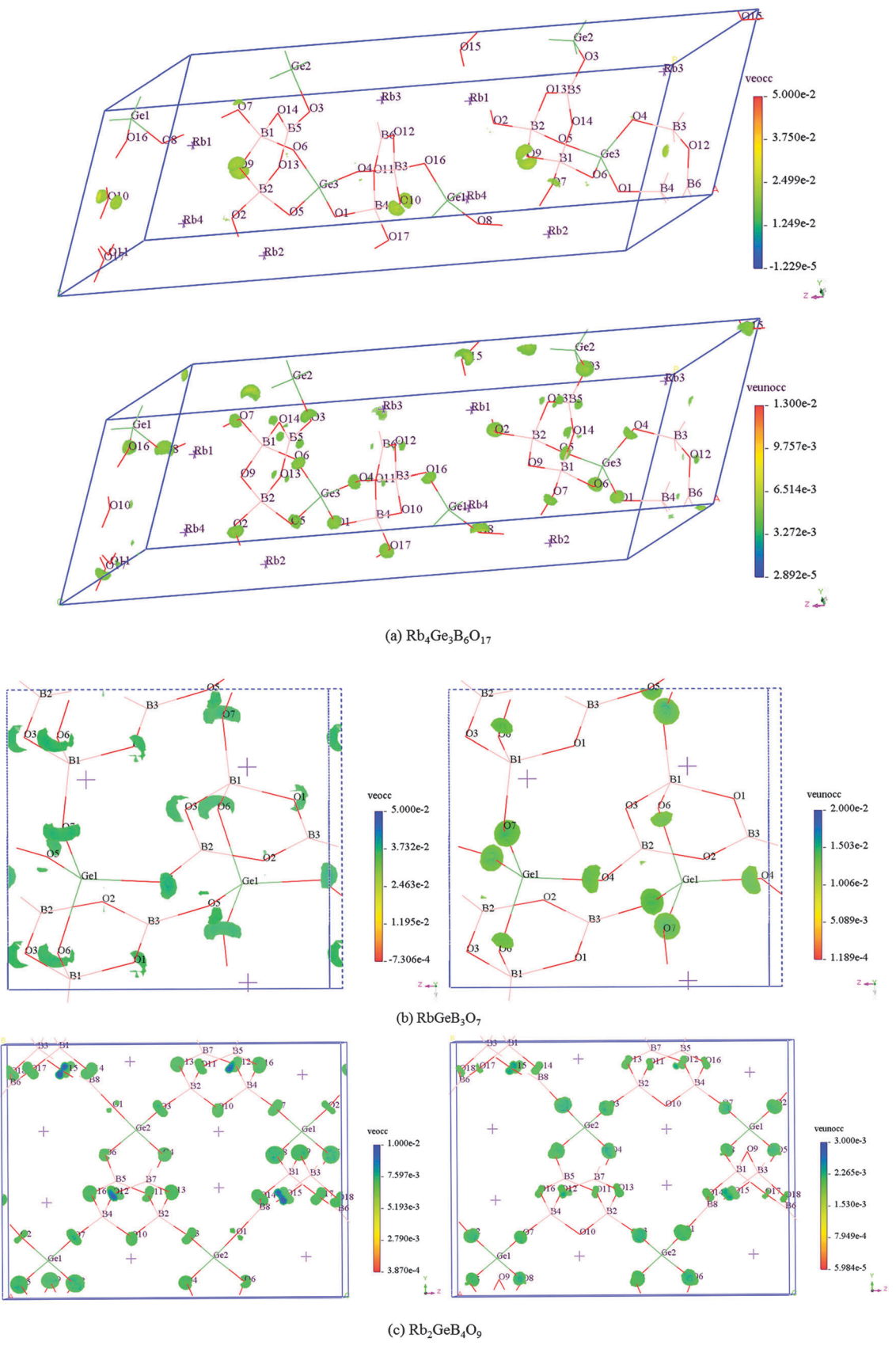
The PDOS of B, Si and Ge are shown in Fig. 3, from which one can see that from the most R-rich case changing to the most B-rich one, the state percentage of B-p orbitals at the top of valence bands tends to grow. The larger percentage of B-p orbitals indicates that, in the region of -5 to 0 eV, the interaction between B/R and O has changed along with the B/R ratio. That is to say, the contributor to the SHG response may be changed with the B/R ratio. From Table 1 we can see that for the B-rich compounds Rb<sub>4</sub>Ge<sub>3</sub>B<sub>6</sub>O<sub>17</sub>, RbGeB<sub>3</sub>O<sub>7</sub> and Rb<sub>2</sub>GeB<sub>4</sub>O<sub>9</sub>, the SHG coefficients are obviously larger than those of the R-rich ones of KBGe<sub>2</sub>O<sub>6</sub> and Li<sub>4</sub>B<sub>4</sub>Si<sub>8</sub>O<sub>24</sub>. Fig. 2 shows the obvious SHG densities of the BO<sub>4</sub> or RO<sub>4</sub> tetrahedra, which imply that the  $\pi$ -conjugation configuration of BO<sub>3</sub> is not the only contributor to the SHG response, especially in the compounds Rb<sub>4</sub>Ge<sub>3</sub>B<sub>6</sub>O<sub>17</sub> and RbGeB<sub>3</sub>O<sub>7</sub>.

The PDOS of the O atoms for Rb<sub>4</sub>Ge<sub>3</sub>B<sub>6</sub>O<sub>17</sub> is shown in Fig. 4a, in which the p orbitals of O9 and O10 (the bridging oxygens of two neighbouring BO<sub>4</sub> groups) occupy the valence-band maximum, meaning that O9 and O10 do contribute to the SHG response. For RbGeB<sub>3</sub>O<sub>7</sub> the PDOS of B, O and Ge,

Table 1 Experimental and calculated linear and non-linear optical properties

| Compounds  | Space<br>group                                | Experimental<br>band gap (eV) | Calculated<br>band gap (eV) | Calculated SHG coefficients (pm V <sup>-1</sup> )     | Experimental powder<br>SHG response | Calculated<br>birefringence |
|--|---|-------------------------------|-----------------------------|---|-------------------------------------|-----------------------------|
| KBGe <sub>2</sub> O <sub>6</sub>                               | P2 <sub>1</sub> 2 <sub>1</sub> 2 <sub>1</sub> |                               | 3.77                        | $d_{14} = -0.340 \text{ (0.87 KDP)}$                  | _                                   | 0.0050                      |
| Li <sub>4</sub> B <sub>4</sub> Si <sub>8</sub> O <sub>24</sub> | $P2_1$  | _                             | 5.51                        | $d_{14} = -0.017, d_{16} = -0.012,$                   | _                                   | 0.0083                      |
|  | •   |                               |                             | $d_{22} = 0.025, d_{23} = 0.028 (0.07 \text{ KDP})$   | 26                                  |                             |
| $LaBSiO_5$   | $P3_1$  | _                             | 5.16                        | $d_{11} = 0.027, d_{15} = 0.002,$                     | $\approx 1 \text{ KDP}^{36}$        | 0.015                       |
|  |   |                               |                             | $d_{22} = -0.385$ (0.99 KDP), $d_{33} = -0.029$       |                                     |                             |
| $LaBGeO_5$   | $P3_1$  | 6.41                          | 4.19                        | $d_{11} = 0.142, d_{15} = 0.236,$                     | 0.33 KDP <sup>29</sup>              | 0.034                       |
|  |   |                               |                             | $d_{22} = -0.179, d_{33} = -0.310 (0.79 \text{ KDP})$ |                                     |                             |
| $Rb_4B_6Ge_3O_{17}$  | Cc  | 5.42                          | 4.33                        | $d_{15} = -0.634$ (1.63 KDP),                         | 1.3 KDP <sup>20</sup>               | 0.0178                      |
|  |   |                               |                             | $d_{24} = 0.390, d_{33} = 0.467$                      |                                     |                             |
| RbGeB <sub>3</sub> O <sub>7</sub>                              | $Pna2_1$                                      | 5.58                          | 4.77                        | $d_{15} = 0.443, d_{24} = 0.694,$                     | 1.3 KDP <sup>20</sup>               | 0.0210                      |
| <i>J</i> ,   | -   |                               |                             | $d_{33} = -0.95 (2.44 \text{ KDP})$                   |                                     |                             |
| Rb <sub>2</sub> GeB <sub>4</sub> O <sub>9</sub>                | $P2_1$  | 5.54                          | 4.27                        | $d_{16} = 0.232, d_{14} = -0.864 (2.22 \text{ KDP}),$ | 2.0 KDP <sup>20</sup>               | 0.0227                      |
| 2 4-3  | •   |                               |                             | $d_{22} = 0.056, d_{23} = -0.173$                     |                                     |                             |

PCCP



 $\textbf{Fig. 2} \quad \textbf{SHG densities of Rb}_4 \textbf{Ge}_3 \textbf{B}_6 \textbf{O}_{17}, \ \textbf{RbGeB}_3 \textbf{O}_7 \ \text{and} \ \textbf{Rb}_2 \textbf{GeB}_4 \textbf{O}_9. \ \textbf{The rainbow represents the activities of the veocc state and veunocc state SHG.}$ 

Paper PCCP

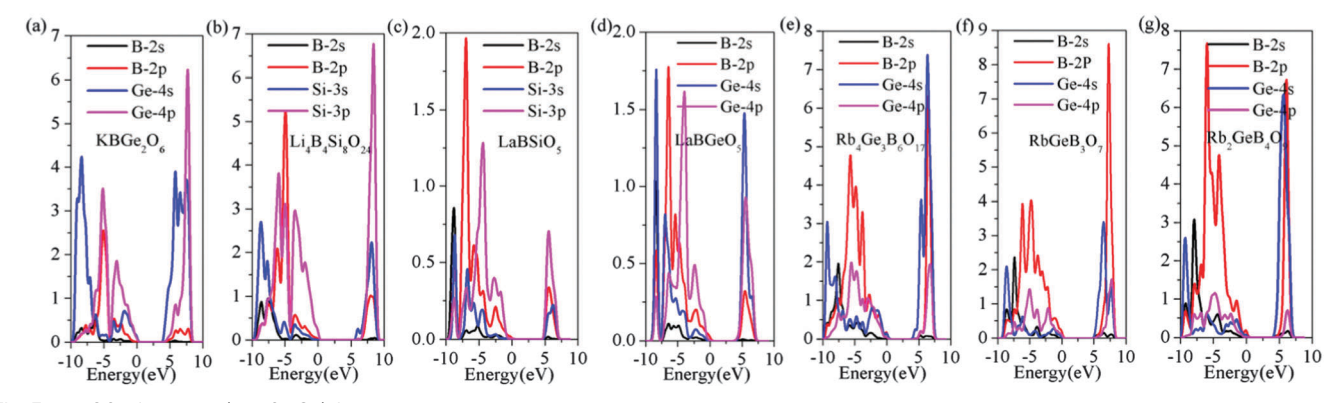


Fig. 3 PDOS of B and R (R = Si, Ge) for the seven structures.

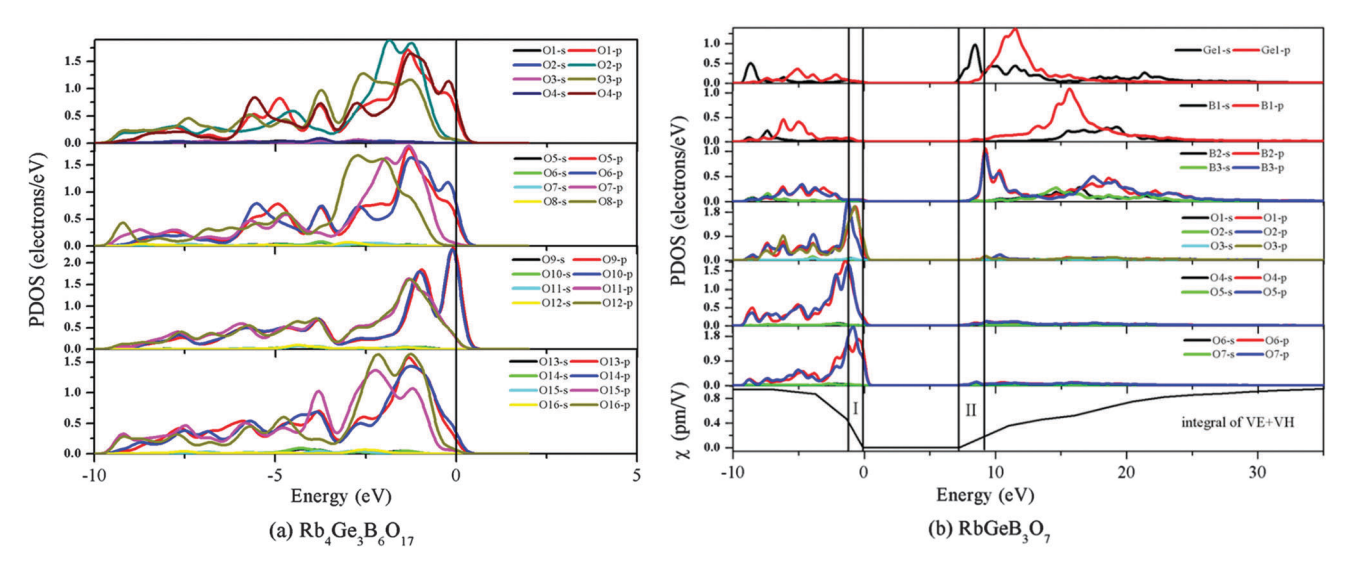


Fig. 4 (a) PDOS of O atoms of the compound  $Rb_4Ge_3B_6O_{17}$ . (b) PDOS of the anionic groups B-O and Ge-O and the integral of VE + VH for compound  $Rb_4Ge_3B_6O_{17}$ .

corresponding to the integral of VE + VH, are given in Fig. 4b. The integral of the band-resolved  $\chi^{(2)}$  increases, corresponding to positive contributions to SHG. One can see that the p orbitals of O1 and O3 (the bridging oxygens of BO<sub>4</sub> and BO<sub>3</sub>), O4 and O5 (the bridging oxygens of GeO<sub>4</sub> and BO<sub>3</sub>), and O6 and O7 (the bridging oxygens of BO<sub>4</sub> and GeO<sub>4</sub>), but not that of O2 (the bridging oxygen of two neighbour BO<sub>3</sub> groups), occupy the main region within -1.30 to 0 eV. That is to say, the nonbonding p orbitals of bridging oxygens occupy the valence-band maximum, which leads to the SHG response of RO<sub>4</sub>. Why does the conjugate  $\pi$  orbital in BO<sub>3</sub> not dominate the top of the valence band as previously expected?

For the trigonal planar  $BO_3$  group, the overlapping p orbitals tend to form  $\pi$  bonds and the amount of non-bonding p orbitals decreases, especially in the two  $BO_3$  groups connected by sharing a vertical oxygen. So the valence-band maximum is mainly occupied by non-bonding p orbitals of tetrahedra, such as  $BO_4$  or  $RO_4$ , which results in the  $\pi$ -conjugated  $BO_3$  group not being the only contributor to SHG, as  $BO_4$  and  $RO_4$  make apparent contributions to SHG (as in the compound RbGeB $_3O_7$ ).

In the structures where  $BO_3$  connects with the  $BO_4$  or  $RO_4$  groups (as in the compounds  $Rb_4Ge_3B_6O_{17}$  and  $Rb_2GeB_4O_9$ ), the  $BO_4$  and  $RO_4$  along with the  $\pi\text{-conjugated}$   $BO_3$  group make equally important contributions to SHG. This implies that, in a structural unit, while the  $\pi\text{-conjugated}$   $BO_3$  group contributes to a larger part of SHG, the contributions of tetrahedral  $BO_4$  and  $RO_4$  cannot be neglected. Furthermore, it also shows that the connection pattern of the anionic group framework is quite important.

#### Conclusions

Using a DFT method, band structure, PDOS and SHG density are analyzed to study the influence of the BBUs on the linear and non-linear optical properties of compounds with different B-R ratios. Based on the SHG density of the seven studied compounds, in the B-rich structures Rb<sub>4</sub>Ge<sub>3</sub>B<sub>6</sub>O<sub>17</sub>, RbGeB<sub>3</sub>O<sub>7</sub> and Rb<sub>2</sub>GeB<sub>4</sub>O<sub>9</sub>, BO<sub>3</sub> is not the only contributor to SHG response. This is because the valence-band maximum is not

occupied only by orbitals of the  $\pi$ -conjugated BO $_3$  group, as the non-bonding p orbitals of the bridging oxygens in BO $_4$  and RO $_4$  are closer to the Fermi level than that of BO $_3$  and tetrahedral BO $_4$  and RO $_4$  noticeably contribute to the SHG response. In summary, the tetrahedra may make a significant contribution to the SHG response of Ge/Si-containing borate crystals, which makes it necessary to study this kind of tetrahedral borate and is meaningful for the design and synthesis of NLO materials with varied structures.

### Acknowledgements

**PCCP** 

This work is supported by National Basic Research Program of China (Grant No. 2014CB648400), the National Natural Science Foundation of China (Grant No. 11265015, 11474353), the Recruitment Program of Global Experts (1000 Talent Plan, Xinjiang Special Program), and the Instrument Developing Project of the Chinese Academy of Sciences (Grant No. YZ201349).

#### Notes and references

- 1 P. Yu, L. M. Wu, L. J. Zhou and L. Chen, *J. Am. Chem. Soc.*, 2014, **136**, 480.
- 2 H. P. Wu, H. W. Yu, Z. H. Yang, X. L. Hou, X. Su, S. L. Pan, K. R. Poeppelmeier and J. M. Rondinelli, *J. Am. Chem. Soc.*, 2013, 135, 4215.
- 3 P. Becker, Adv. Mater., 1998, 10, 979.
- 4 J. Lin, M. H. Lee, Z. P. Liu, C. T. Chen and C. J. Pickard, *Phys. Rev. B: Condens. Matter Mater. Phys.*, 1999, **60**, 13380.
- C. T. Chen, Y. C. Wu, A. D. Jiang, B. C. Wu, G. M. You,
   R. K. Li and S. J. Lin, J. Opt. Soc. Am. B, 1989, 6, 616.
- 6 Y. Mori, I. Kuroda, S. Nakajima, T. Sasaki and S. Nakai, *Appl. Phys. Lett.*, 1995, **67**, 1818.
- 7 H. Zhang, M. Zhang, S. L. Pan, X. Y. Dong, Z. H. Yang, X. L. Hou, Z. Wang, K. B. Chang and K. R. Poeppelmeier, J. Am. Chem. Soc., 2015, 137, 8360.
- 8 M. C. Chen, L. M. Wu, H. Lin, L. J. Zhou and L. Chen, J. Am. Chem. Soc., 2012, 134, 6058.
- H. P. Wu, S. L. Pan, K. R. Poeppelmeier, H. Y. Li, D. Z. Jia,
   Z. H. Chen, X. Y. Fan, Y. Yang, J. M. Rondinelli and
   H. S. Luo, J. Am. Chem. Soc., 2011, 133, 16317.
- C. T. Chen, Y. C. Wu and R. K. Li, *Int. Rev. Phys. Chem.*, 2008, 8, 65.
- 11 J. L. Song, C. L. Hu, X. Xu, F. Kong and J. G. Mao, *Angew. Chem., Int. Ed.*, 2015, 54, 3679.
- 12 X. Su, Z. H. Yang, M. H. Lee, S. L. Pan, Y. Wang, X. Y. Fan, Z. J. Huang and B. B. Zhang, *Phys. Chem. Chem. Phys.*, 2015, 17, 5338.
- J. J. Zhang, Z. H. Zhang, W. G. Zhang, Q. X. Zheng, Y. X. Sun,
   C. Q. Zhang and X. T. Tao, *Chem. Mater.*, 2011, 23, 3752.
- 14 H. S. Ra, K. M. Ok and P. S. Halasyamani, *J. Am. Chem. Soc.*, 2003, **125**, 7764.
- X. Su, Y. Wang, Z. H. Yang, X. C. Huang, S. L. Pan, F. Li and M. H. Lee, *J. Phys. Chem. C*, 2013, 117, 14149.

- 16 Y. Z. Huang, L. M. Wu, X. T. Wu, L. H. Li, L. Chen and Y. F. Zhang, J. Am. Chem. Soc., 2010, 132, 12788.
- 17 M. M. Li, Y. Dai, X. C. Ma, Z. J. Li and B. B. Huang, *Phys. Chem. Chem. Phys.*, 2015, 17, 17710.
- 18 W. J. Yao, R. He, X. Y. Wang, Z. S. Lin and C. T. Chen, *Adv. Opt. Mater.*, 2014, 2, 411.
- 19 K. Xu, P. Loiseau and G. Aka, *J. Cryst. Growth*, 2009, 311, 2508.
- 20 J. H. Zhang, C. L. Hu, X. Xu, F. Kong and J. G. Mao, *Inorg. Chem.*, 2011, 50, 1973.
- 21 F. Kong, H. L. Jiang, T. Hu and J. G. Mao, *Inorg. Chem.*, 2008, 47, 10611.
- 22 Z. E. Lin, J. Zhang and G. Y. Yang, *Inorg. Chem.*, 2003, 42, 1797.
- 23 V. I. Gavrilenko, R. Q. Wu, M. C. Downer, J. G. Ekerdt, D. Lim and P. Parkinson, *Phys. Rev. B: Condens. Matter Mater. Phys.*, 2001, 63, 165325.
- 24 D. Lim, M. C. Downer, J. G. Ekerdt, N. Arzate, B. S. Mendoza, V. I. Gavrilenko and R. Q. Wu, *Phys. Rev. Lett.*, 2000, 84, 3406.
- 25 J. B. P. T. E. Gier, Chem. Mater., 1992, 4, 1065.
- 26 X. Xu, C. L. Hu, F. Kong, J. H. Zhang, J. G. Mao and J. Sun, *Inorg. Chem.*, 2013, 52, 5831.
- 27 H. P. Wu, H. W. Yu, S. L. Pan, Z. J. Huang, Z. H. Yang, X. Su and K. R. Poeppelmeier, *Angew. Chem., Int. Ed.*, 2013, 52, 3406.
- 28 Y. Takahashi, Y. Benino, T. Fujiwara and T. Komatsu, *J. Appl. Phys.*, 2001, **89**, 5282.
- 29 Y. Takahashi, Y. Benino, T. Fujiwara and T. Komatsu, *Jpn. J. Appl. Phys.*, 2002, **41**, L1455.
- 30 Y. Takahashi, Y. Benino, V. Dimitrov and T. Komatsu, *J. Non-Cryst. Solids*, 1999, **260**, 155.
- 31 O. A. Gurbanova and E. L. Belokoneva, *Crystallogr. Rep.*, 2007, 52, 624.
- 32 E. L. Belokoneva, W. I. F. David, J. B. Forsyth and K. S. Knight, *J. Phys.: Condens. Matter*, 1997, **9**, 3503.
- 33 L. S. Chi, H. Y. Chen, H. H. Zhuang and J. S. Huang, J. Alloys Compd., 1997, 252, L12.
- 34 J. B. Parise and T. E. Gier, Int. J. Inorg. Mater., 2000, 2, 81.
- 35 Z. H. Li, Z. H. Lin, Y. C. Wu, P. Z. Fu, Z. Z. Wang and C. T. Chen, *Chem. Mater.*, 2004, **16**, 2906.
- 36 L. P. Li, Q. Jing, Z. H. Yang, X. Su, B.-H. Lei, S. L. Pan, F. F. Zhang and J. Zhang, J. Appl. Phys., 2015, 118, 113104.
- 37 B.-H. Lei, Q. Jing, Z. H. Yang, B. B. Zhang and S. L. Pan, J. Mater. Chem. C, 2015, 3, 1557.
- 38 S. J. Clark, M. D. Segall, C. J. Pickard, P. J. Hasnip, M. J. Probert, K. Refson and M. C. Payne, *Z. Kristallogr.*, 2005, 220, 567.
- 39 B. G. Pfrommer, M. Cote, S. G. Louie and M. L. Cohen, *J. Comput. Phys.*, 1996, **131**, 231.
- 40 J. P. Perdew, K. Burke and M. Ernzerhof, *Phys. Rev. Lett.*, 1996, 77, 3865.
- 41 D. Vanderbilt, *Phys. Rev. B: Condens. Matter Mater. Phys.*, 1990, **41**, 7892.
- 42 C. S. Wang and B. M. Klein, *Phys. Rev. B: Condens. Matter Mater. Phys.*, 1981, **24**, 3417.
- 43 R. W. Godby, M. Schlüter and L. J. Sham, *Phys. Rev. B: Condens. Matter Mater. Phys.*, 1988, 37, 10159.

- 44 Q. Jing, X. Y. Dong, Z. H. Yang, S. L. Pan, B. B. Zhang, X. C. Huang and M. W. Chen, J. Solid State Chem., 2014, 219, 138.
- 45 C. Aversa and J. E. Sipe, *Phys. Rev. B: Condens. Matter Mater. Phys.*, 1995, 52, 14636.
- 46 B. B. Zhang, M. H. Lee, Z. H. Yang, Q. Jing, S. L. Pan, M. Zhang, H. P. Wu, X. Su and C. S. Li, *Appl. Phys. Lett.*, 2015, 106, 031906.
- 47 B. B. Zhang, Z. H. Yang, Y. Yang, M.-H. Lee, S. L. Pan, Q. Jing and X. Su, *J. Mater. Chem. C*, 2014, 2, 4133.
- 48 M. H. Lee, C. H. Yang and J. H. Jan, *Phys. Rev. B: Condens. Matter Mater. Phys.*, 2004, **70**, 235110.
- 49 C.-H. Lo, Master thesis, Tamkang University, 2005.
- 50 Z. S. Lin, L. Kang, T. Zheng, R. He, H. Huang and C. T. Chen, *Comput. Mater. Sci.*, 2012, **60**, 99.
- 51 Q. Bian, Z. H. Yang, L. Y. Dong, S. L. Pan, H. Zhang, H. P. Wu, H. W. Yu, W. W. Zhao and Q. Jing, J. Phys. Chem. C, 2014, 118, 25651.
- 52 C. T. Chen, G. L. Wang, X. Y. Wang and Z. Y. Xu, *Appl. Phys. B: Lasers Opt.*, 2009, **97**, 9.